REPORT DOCUMENTATION PAGE

Form Approved
OMB No. 0704-0188

PLEASE DO NOT RETURN YOUR FORM TO THE ABOVE ORGANIZATION.

1. REPORT DATE *(DD-MM-YYYY)*	2. REPORT TYPE	3. DATES COVERED *(From - To)*
20-08-2012	Final	03/01/2009-11/30/2011

4. TITLE AND SUBTITLE
"(YIP) Multifunctional Ultra-Light Mg-Li Alloy Nanocomposites"

5a. CONTRACT NUMBER

5b. GRANT NUMBER
FA9550-09-1-0151

5c. PROGRAM ELEMENT NUMBER

6. AUTHOR(S)
Gleb Yushin

5d. PROJECT NUMBER

5e. TASK NUMBER

5f. WORK UNIT NUMBER

7. PERFORMING ORGANIZATION NAME(S) AND ADDRESS(ES)
Georgia Institute of Technology
School of Materials Science & Engineering
771 Ferst Dr. NW, Atlanta, GA 30332

8. PERFORMING ORGANIZATION REPORT NUMBER

9. SPONSORING/MONITORING AGENCY NAME(S) AND ADDRESS(ES)
AFOSR
875 N. Randolph Street
Arlington, VA 22203
Program Manager: Dr. Byung-Lip Lee, AFOSR/NA

10. SPONSOR/MONITOR'S ACRONYM(S)

11. SPONSOR/MONITOR'S REPORT NUMBER(S)
AFRL-OSR-VA-TR-2012-1114

12. DISTRIBUTION/AVAILABILITY STATEMENT
Distribution A: Approved for Public Release

13. SUPPLEMENTARY NOTES

14. ABSTRACT

Magnesium-lithium (Mg-Li) alloys are attractive lightweight materials for many structural components of aircraft due to their high strength-to-weight ratio. They are also attractive as Li-ion battery anodes due to their high capacity and long lifetime. This multi-functionality may allow a Mg-Li airframe to serve as an energy source or peak power source for various aerial vehicles. Micro-crystalline Mg-Li alloys prepared using classical metallurgy methods exhibit low fracture toughness. Amorphous and nanocrystalline Mg-Li alloys are expected not to have this limitation. However, they have never been produced and investigated. We proposed to perform such an investigation and additionally synthesize a novel ultra-light high strength material with high energy / high power electrical energy storage capability based on a Mg-Li with carbon fiber reinforcements. .

15. SUBJECT TERMS

16. SECURITY CLASSIFICATION OF:			17. LIMITATION OF ABSTRACT	18. NUMBER OF PAGES	19a. NAME OF RESPONSIBLE PERSON
a. REPORT	b. ABSTRACT	c. THIS PAGE			19b. TELEPHONE NUMBER *(Include area code)*
U	U	U	U		

Reset

Final report: **(YIP-09) Multifunctional Ultra-Light Mg-Li Alloy Nanocomposites**

AFOSR: FA9550-09-1-0151; Start date: March, 1st, 2009

Gleb Yushin, Georgia Institute of Technology
School of Materials Science & Engineering
Phone: (404) 385 - 3261; Email: yushin@gatech.edu

Directorate: Aerospace. & Materials Science

Research Area: Mechanics of Multifunctional Materials & Microsystems

Attn: Dr. Byung-Lip Lee, AFOSR/NA, (703) 696-8483, byung-lip.lee@afosr.af.mil

1. Contributors to this project

James Benson (Ph.D. student), Dr. Igor Kovalenko, Dr. Alexandre Magasinski, Kara Evanoff (Ph.D. student)

2. Publications and presentations

2.1. International meetings

1. G. Yushin, *Nanostructured Materials for Energy Storage Application*s, GORDON Research Conference (GRC) on Electrochemistry taken place in Ventura, CA (2012) **(invited)**
2. G. Yushin, *Nanoccomposite Materials for Energy Storage and Multifunctional Application*s at TMS, Orlando, FL (2012) **(invited)**
3. G. Yushin, *Nanocomposite Materials for Energy Storage Application*s, Conference on Electronic Materials and Applications (EMA 2012), session Advanced Energy Storage Materials and Systems: Lithium and Beyond **(invited)**
4. G. Yushin, *Nanocomposite Carbon-Containing Materials for Energy Storage and Multifunctional Application*s, at the Workshop on "Carbon Materials for Energy" organized by Fraunhofer IWS, Dresden, Germany (**a keynote lecture)**.
5. G. Yushin, *Nanocomposite Materials for High Energy Supercapacitors and Li-ion Batteries*, at the 1st NSF-sponsored US-Taiwain Workshop for Materials and Systems "Challenges in Electrical Energy Storage", Taipei, Taiwan (2011) **(invited)**
6. G. Yushin, *Nanostructured Materials for Energy Storage Application*s, at the 10X Advanced Battery R&D Conference, Santa Clara, CA, USA (2011) **(invited)**
7. K. Evanoff, T. Fuller, J. Ready, and G. Yushin, *Silicon Coated Vertically Aligned Carbon Nanotubes as High Capacity Anodes for Lithium Ion Batteries* MRS Spring Meeting, San Francisco, CA (2011).

8. G. Yushin, *Nanostructured Materials for Energy Storage Application*s, at the 10X Advanced Battery R&D Conference, which took place in Santa Clara, CA, USA (2010) **(invited)**
9. G. Yushin, *Nanocomposite Materials for Energy Storage Applications,* at the 2nd UNIST International Conference, which took place in Ulsan, Korea (2010) **(invited)**
10. B. Hertzberg, S. Boukhalfa, A. Magasinski, I. Kovalenko, P. Dixon, and G. Yushin, *Carbon-Containing Nanocomposite Materials for Energy Storage*, American Chemical Society, Boston, MA (2010) **(invited)**.
11. G. Yushin, *Latest Developments in Anode Technologies*, National Alliance for Advanced Technology Batteries, webinar (2010) **(invited)**.
12. K. Evanoff, B. Hertzberg, T.F. Fuller, W.J. Ready, G. Yushin, *Silicon-Decorated Carbon Nanotubes as High Capacity Anodes for Lithium Ion Batteries*, 2010 World Conference on Carbon, Clemson, SC (2010)
13. *G. Yushin, Novel materials for advanced supercapacitors and Li-ion batteries,* SES09 Meeting of the American Physical Society, Nov. 13, Atlanta, GA (2009) (**invited**)

2.2. Papers submitted or in preparation

1. Kara Evanoff, Jim Benson, Mark Schauer, Igor Kovalenko, David Lashmore, W. Jud Ready, and Gleb Yushin, "Ultra-Strong Silicon-Coated Carbon Nanotube Nonwoven Fabric as Multifunctional Lithium Ion Battery Anodes", in review at Advanced Energy Materials (2012)

2. J. Benson, S. Baukhalfe, A. Magasinski & G. Yushin, "Chemical Vapor Deposition of Aluminum Nanowires on Metal Substrates for Electrical Energy Storage Applications", ACS Nano (2011)

3. J. Benson, I. Kovalenko, B. Hertzberg, A. Kvit, & G. Yushin, "Electrochemically-Driven Grain Refinement and Amorphization of Al-Li Alloys", in preparation (2012)

4. J. Benson, I. Kovalenko, A. Magasinski & G. Yushin, "Stability of Mg-C Anodes for use in Li-ion Batteries", in preparation for Advanced Energy Materials (2012)

3. Introduction

Multifunctional materials capable of providing an energy storage coupled with a load bearing ability are attractive for applications in which reducing the overall mass and volume of equipment is important, such as unmanned or aerospace vehicles [1-4], tents and outdoor special clothing for turists going for long trips, professionals going to expiditions and solders going for missions. Flexible Li-ion batteries with load bearing abilities could be attractive candidates for these applications due to their high energy and power densities. As a first step towards

realization of such a battery design one needs to develop scalable synthesis routes to produce structural and flexible anodes and cathodes.

Magnesium-lithium (Mg-Li), aluminum-lithium (Al-Li) and silicon-lithium (Si-Li) alloys are attractive lightweight materials for both structural aircraft components and Li-ion battery anodes. This multi-functionality may allow the airframe to serve as a power/energy source for a variety of applications, including hybrid engines for combat aerial vehicles.

4. Goals for the project

- Systematic studies of the effects of electrochemical parameters on Mg-, Al- and Si-alloy microstructure

- Fabrication of porous ultra-light high strength carbon-containing composite materials (Mg/C, Al/C, Si/C) with high energy / high power electrical energy storage capability

5. Results and Discussion

5.1. Microstructure Modification

Figure 1 Shows a typical XRD response from lithiating aluminum samples. By comparing to standard data collected we have shown the formation of AlLi crystalline phase which can be seen in Figure 2.

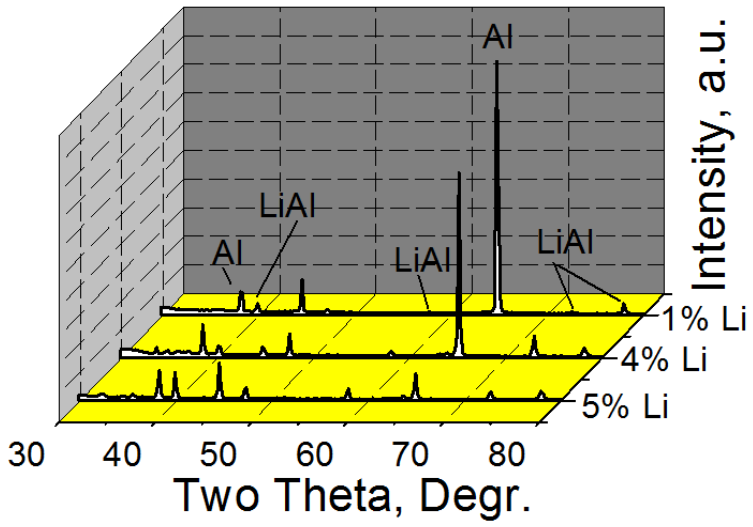

Fig.1. *X-ray diffraction experiments: changes in the Al sheet microstructure upon electrochemical alloying with Li*

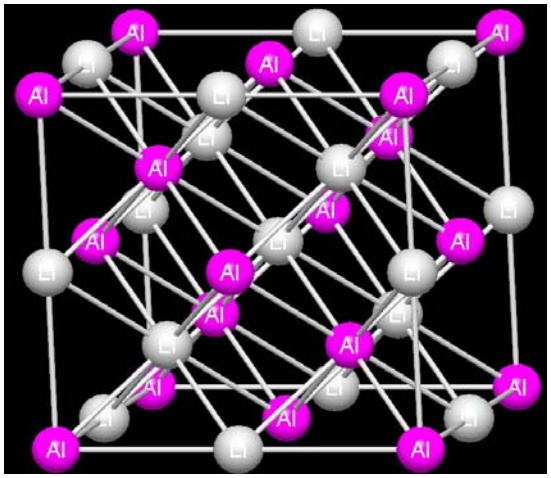

Fig.2. *Crystal structure of perfect stoichiometric AlLi observed in XRD experiments.*

To determine the effects of increasing amount of lithiation on the grain size we used aluminum 1030 sheet and made coin cells after annealing in air for 2 hrs at 500 C and polishing in the dry, argon filled glovebox. As seen in Figure 3 the aluminum grain size reduces instantaneously from the annealed condition (shown here as >500 nm) while the AlLi grain size approaches the same value of 50 nm. This order of magnitude reduction of grain size has a significant effect on the strength (Fig. 4) and hardness (Fig. 5) of the aluminum.

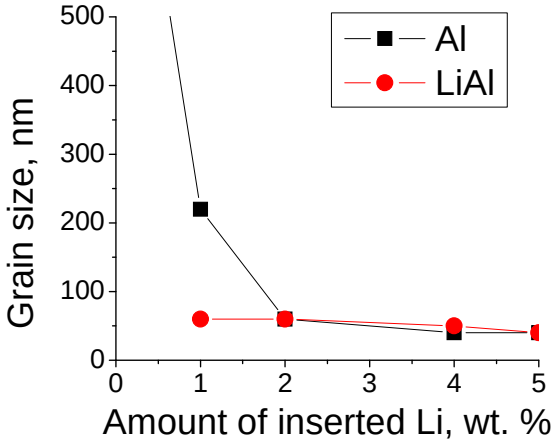

Fig. 3. *Changes in Al grain size upon electrochemical alloying of Al sheet with Li at room temperature. The grain size of the formed LiAl phase is also provided.*

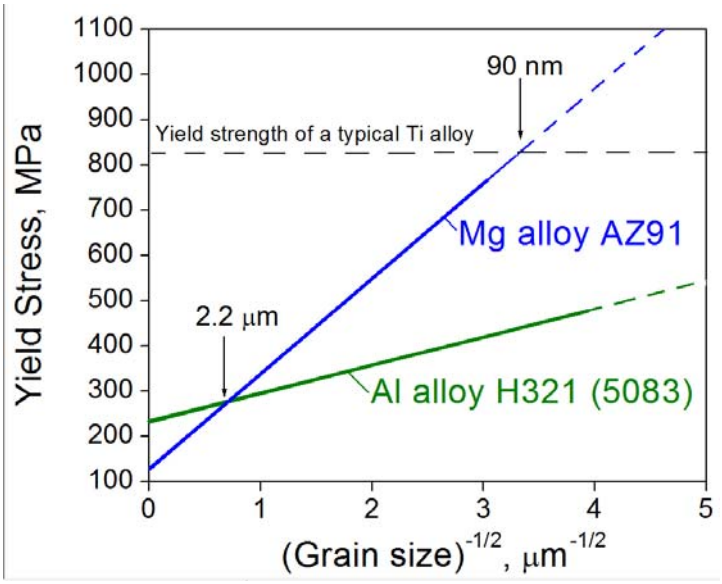

Fig.4. *Yield Stress in Al and Mg alloys as a function of the grain size.*

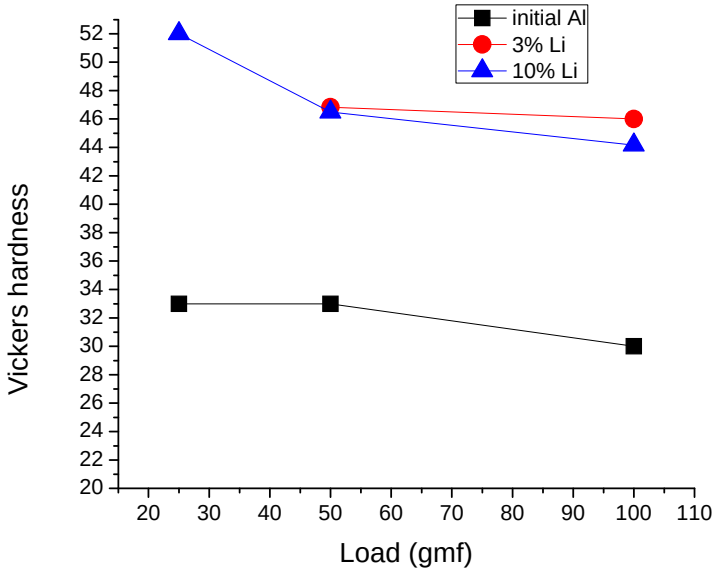

Fig.5. *Hardness of Al before and after Li insertion and the resulting grain size reduction.*

5.2. Electrochemical Performance of C-Al Composite as Anodes for Li-ion Batteries

Electrodes' specific capacity determines the energy storage characteristics of Li-ion batteries. The high specific capacity of C-Al composite electrodes (Fig. 6) is beneficial for energy storage capabilities of the multifunctional material under study.

During the lifetime of a battery many parameters may affect the performance. In aluminum systems one of the greatest inhibitor of cycle stability is the large volume change which occurs during lithiation. This repeated volume change leads to an increased surface area by refining of the particles and the resulting loss of electrical paths within the electrode. The use of nanostructured electrodes is believed to be required for successful implementation of the Li-alloy anodes[5].

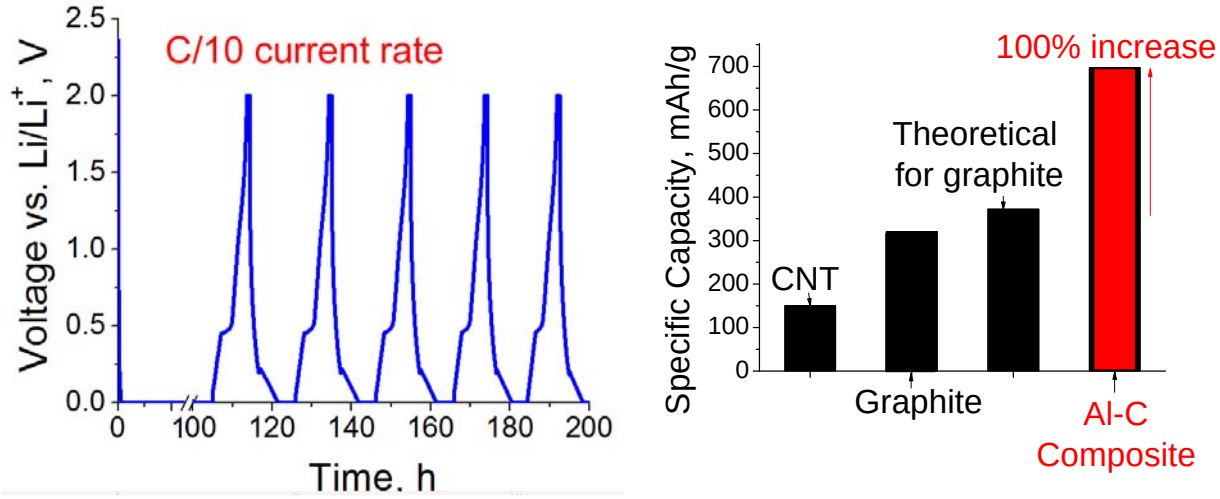

Fig.6. *Voltage profiles (left) and specific capacity of Al-C composite electrodes.*

5.3. Electrochemical Performance of C-Mg Composite as Anodes for Li-ion Batteries

Initial attempts to lithiate (insert Li ions into) Mg powder was inhibited by the formation of a dense, ionically non-conducting native oxide layer. This problem was evident in our first charge discharge studies performed on magnesium powder electrodes prepared outside of the glovebox. These batteries seemed to show very low capacities (less than 40 mAh/g – compared to 300-360 mAh/g for graphite). In this case the native oxide film on the magnesium powder prevented the lithiation of the magnesium particles and forced the lithium ions into the PureBLACK particles (18 wt%) providing for a small amount of capacity. Thus the good cycle stability was due to PureBLACK only.

However, by performing mechanochemical activation by ball-milling Mg and PureBLACK powder in a vacuum-seal container we successfully removed the native oxide in Mg and produced highly active composite electrode (Figure 7) with 2 times higher specific capacity than traditional graphite (Figs 8-11).

We found that both salt and solvent in an electrolyte plays an important role in the capacity and stability of the Mg-C based anodes. For example, while in some electrolytes (Figures 8-10) Mg-C composites exhibit moderately high capacity (600-650 mAh/g) and good stability, in others (e.g. Figure 11) Mg-C may initially exhibit higher capacity (up to 1100 mAh/g) but undergo very rapid degradation and show uncontrolled elechtrochemical reactions, as demonstrated by higher discharge capacities than charge capacities (Figure 11).

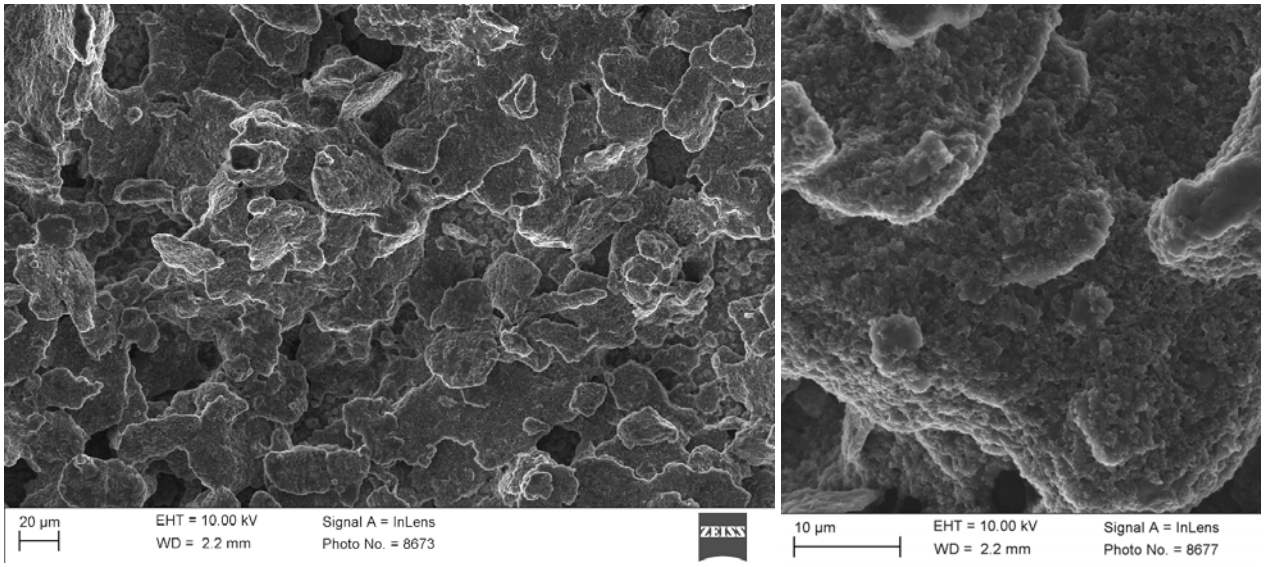

Fig. 7. SEM micrographs of a typical chemo-mechanically activated C-Mg composite electrode used in the studies

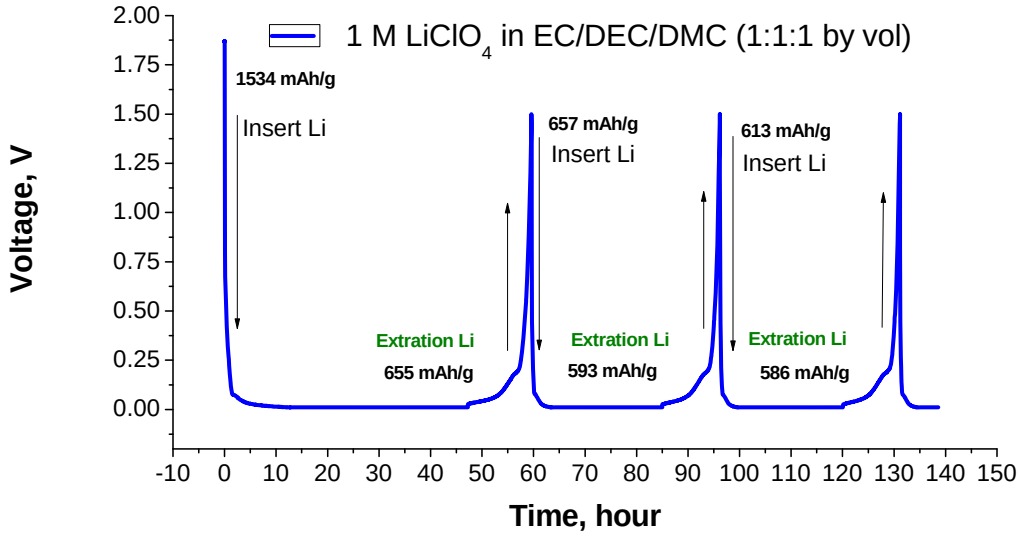

Fig. 8. A typical room-temperature charge-discharge profile of Mg-C composite anode for a Li-ion battery

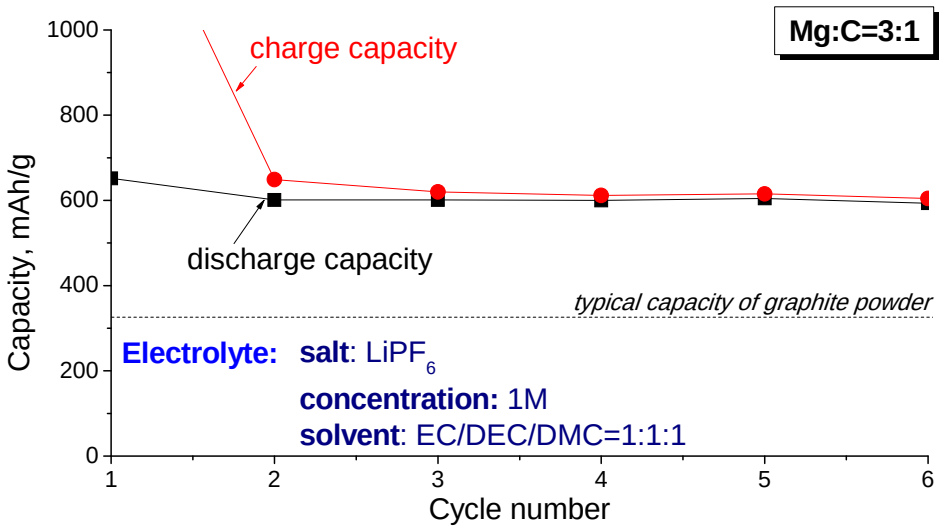

Fig. 9. Room temperature charge and discharge capacity of the mechano-chemically activated Mg-C composite in 1M $LiPF_6$ EC/DEC/DMC electrolyte solution.

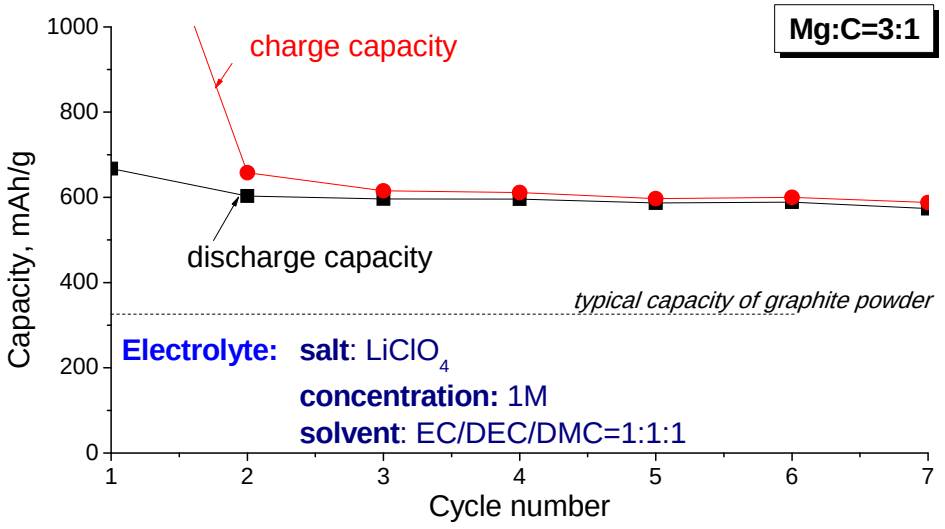

Fig. 10. Room temperature charge and discharge capacity of the mechano-chemically activated Mg-C composite in 1M $LiClO_4$ EC/DEC/DMC electrolyte solution.

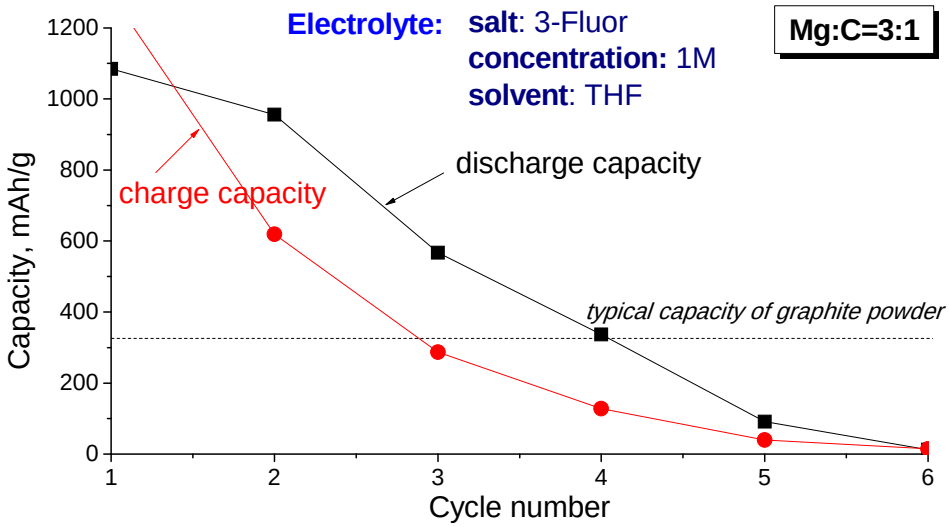

Fig. 12. Room temperature charge and discharge capacity of the mechano-chemically activated Mg-C composite in 1M $LiPF_6$ in THF electrolyte solution.

5.4. Li-ion insertion into Mg foils

Very slow diffusion of Li was also observed in Mg sheet (Mg foils). Even when charging current was as low as 0.3 mA/cm^2 the voltage immediately drops to below 0 V vs Li/Li+. The low discharge capacity can be seen in Figure 13. The oxide layer adheres very well to the foil and can accommodate the stresses generated due to lithiation. To circumvent this problem the oxide layer on Mg sheets was mechanically removed in an Ar-filled glove box (Figure 14). This process was found to dramatically enhance electrochemical activity of the Mg and Mg alloy (ZA31) sheets, as evident from cyclic voltametry studies. Scans were done starting at open circuit potential and going to 0.01 V vs Li at scan rates of 0.5 mV/s, 0.1 mV/s, and 0.02 mV/s, and temperatures of room temp, 40, 60 and 70 °C to study the possibility of repassivation as well as extraneous electrochemical reactions. The charge discharge studies discussed above were repeated with unpassivated magnesium at 0.3, 0.2, and 0.1 mA/cm^2. As expected, higher temperatures increased the reaction kinetics for the 40 °C and 60 °C samples as seen by the increased peak heights, however the higher temperature also destabilized the solid electrolyte interphase (SEI) in the higher voltage potential region as seen by the large peaks above 1.5 V shown in Figure 15. The SEI stability was not observed to cause electrode degradation for 40 °C magnesium alloy (AZ31) electrodes as shown by the cycle stability in Figure 16. The two deintercalation peaks observed for the cyclic voltametry (Fig. 16) could be due to the presence of Al in the AZ31 alloy sheets (3 wt. %). Our prior research showed that the deintercalation peak of aluminum occurs at 0.47 V vs Li/Li+, suggesting that the intercalation of oxide free magnesium in carbonate solutions to occur at 0.2 V vs Li/Li+. With the oxide layer removed the magnesium batteries were finally able to be electrochemically active and charging was achieved.

Constant voltage lithiation of powder and metallic electrodes was performed in order to provide control over what phases could form. In addition high temperature was used to speed up the lithiation process and then compared with room temperature performance to determine the advantages of modest temperature changes. Figure 17 shows the results of moderate voltages used to insert lithium into the magnesium electrodes. High capacities were achieved for the powder electrode (with in excess of 50 % of

the total theoretical lithiation could be attained at 70 °C). This high temperature (70 ºC) increases the lithiation capacity of the thin sheets (200 um) by over 4.3 times, as compared to room temperature studies.

As current methods of removing oxide film rely on the uniformity of mechanical removal, and are subject to some degree of variability, electrochemical methods are also being pursued. Activating agents could be used with magnesium to form catalysis reagents and by employing these activating agents to the electrolyte the passivation tendencies of magnesium will be reduced. This will be even more important for powder electrodes where the high surface area can provide more opportunities for oxidation and complete removal of these films is much more difficult to ensure. Current activating agents include $HgCl_2$, $PbCl_2$, and $InCl_3$.

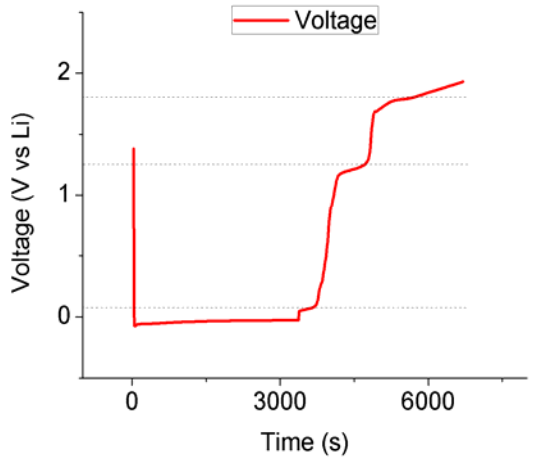

Fig. 13. Room temperature charge/discharge of Mg alloy (AZ31) having a native oxide layer at the current density of 0.3 mA/cm^2.

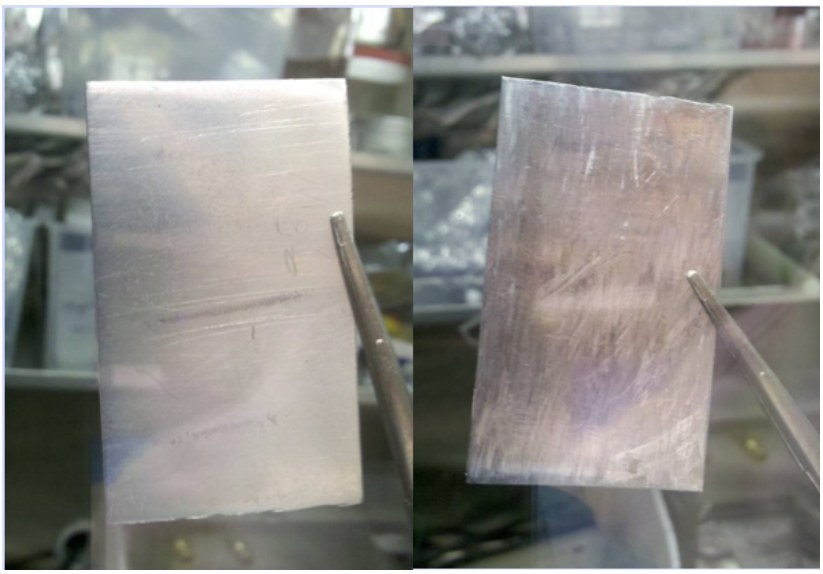

Fig. 14. Mg alloy (AZ31) sheet before (left) and after (right) activation by mechanically removing the surface oxide film with a razor inside an argon glovebox.

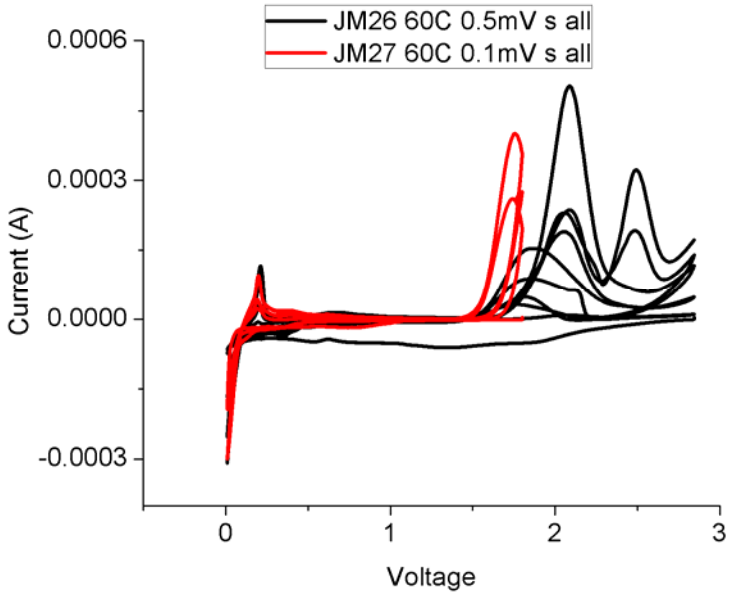

Fig. 15. Cyclic voltammetry of magnesium sheet at 60 ºC at scan rates of 0.5 mV/s and 0.1 mV/s showing unstable SEI films above 1.5V as well as lithium intercalation at lower potentials.

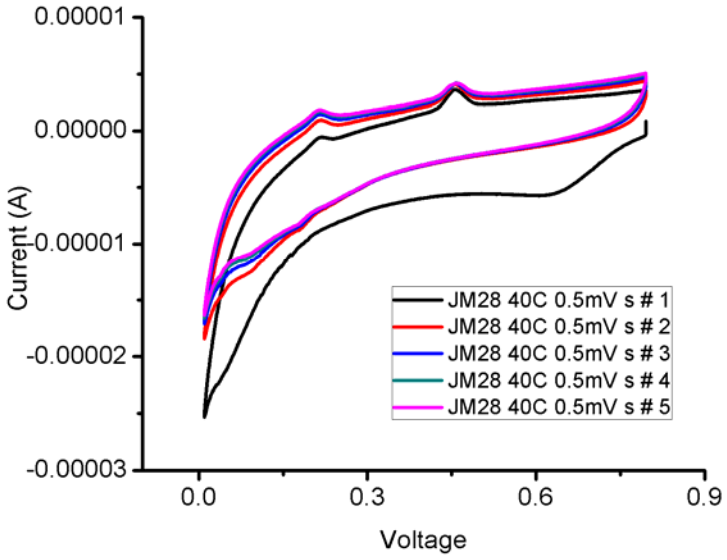

Fig. 16. Cyclic voltammetry of Mg alloy (AZ 31) sheet in Li-ion half cell tested at 40 C and 0.5 mV/s scan rate. Good cycle stability as well as deintercalation peaks for magnesium and aluminum at 0.2 and 0.47 V, respectively, are clearly visible.

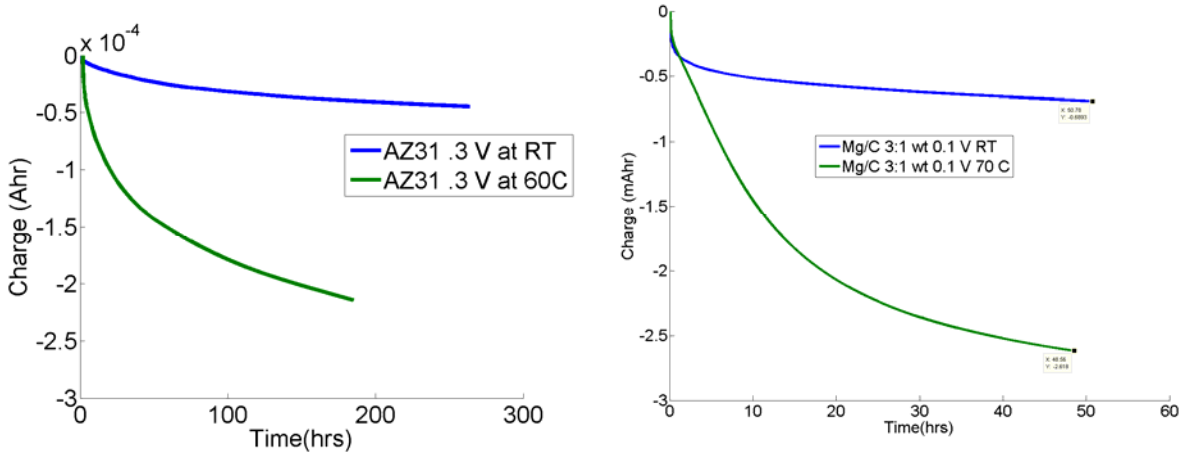

Fig. 17. Effect of temperature on Li+ ion diffusion into Mg: constant voltage charge of Mg alloy (AZ31) foil (left) and Mg-C composite (Mg:C=3:1) powder (right) electrodes at 0.3 V and 0.1 V vs. Li/Li+ at room temperature (RT) and at 70 ºC, showing 3-5 times faster ion transport at elevated temperatures.

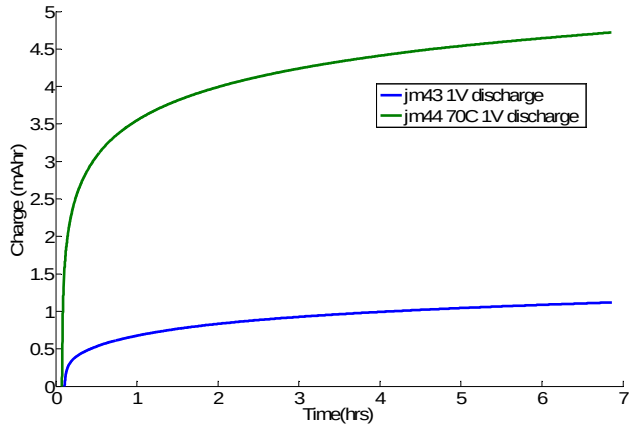

Fig. 18. Effect of temperature on Li+ ion diffusion from Li-Mg: constant voltage (1 V vs. Li/Li+) discharge of Mg-C composite (Mg:C=3:1) powder electrodes a at room temperature (RT) and at 70 ºC, showing 3-5 times faster ion transport at elevated temperatures.

5.5. Multifunctional Si-CNT Composite Anodes

The traditional technique to fabricate electrodes requires mixing of the active particles with carbon conductive additives and a polymer binder and then casting the mixture onto metal foil or mesh current collectors (Figure 19a). Due to point contact between the individual particles, electrical and thermal conductivities of such traditional electrodes are quite limited [6]. The tensile strength of the traditional electrodes is practically governed by the mechanical properties of the metail foil current collectors, because the particles in the electrode are bonded very weekly. Another disadvantage of the traditional electrodes is the significant weight of the metal current collectors, which further limits the gravimetric capacities of the battery cells. For example, while the commercial graphites exhibit capacities in the range of 300-360 $mAh \cdot g^{-1}$ and the weight of the binder and carbon additives is limited to only 10-15 wt. %, the effective capacities of Li-ion battery anodes is commonly less than 200 $mAh \cdot g^{-1}$ if all the materials including heavy Cu foil are taken into account. Indeed, the weight of the Cu foil accounts for over 35 % of the total weight. If high capacity Li-alloying materials such as silicon (Si) are used to improve the gravimetric energy density of Li-ion batteries [7-20], then the relative weight of the Cu foil may account for up to 80 wt. %.

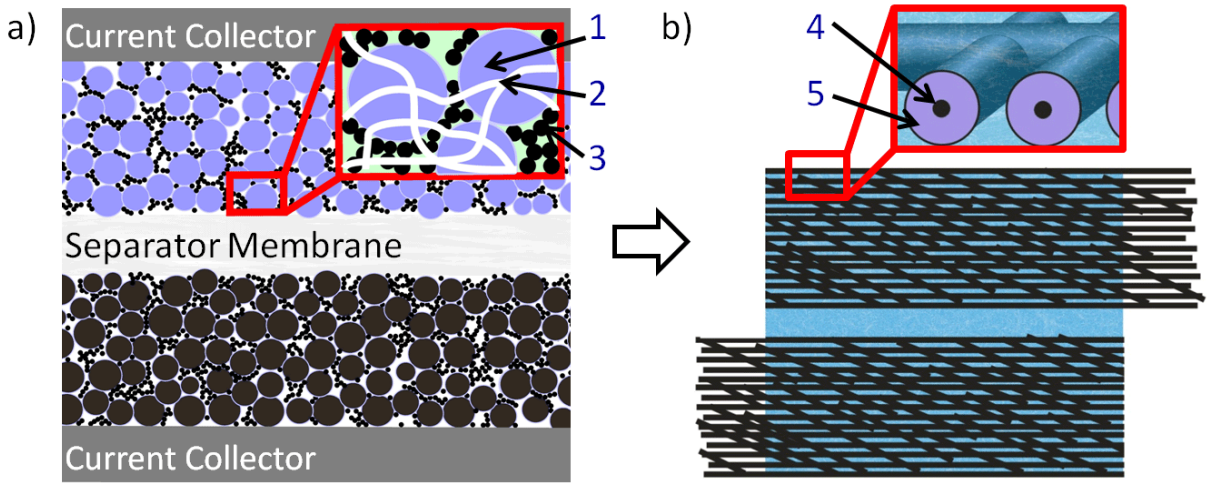

Fig 19. Schematics of elementary Li-ion battery units for (a) traditional and (b) proposed architectures. In a traditional architecture the electrodes, composed of active powders (1), polymer binder (2) and conductive carbon additives, are cast on metal current collector foils. In a proposed architecture the CNT fabric (4) coated with active material layers (5) serves as lightweight multi-functional current collectors for both anodes and cathodes.

Various approaches to fabricate structural electrodes to enhance the mechanical properties have been reported in the literature. Following traditional electrode fabrication techniques, a previous study combined $LiCoO_2$ particles, carbon additives, and polymer binder into a slurry and measured a maximum tensile strength < 5 MPa, a value which may limit widespread applicability of this technique to provide structural support due to the low polymer binder strength and its low content.[2] Sintered composite particle-based electrodes

demonstrated increased strength (~90 MPa) however the capacity retention over 10 cycles was very poor with only 85 % of the theoretical capacity retained.[3] In addition, the sintered electrodes are not flexible, which may limit some of their multi-functional applications.

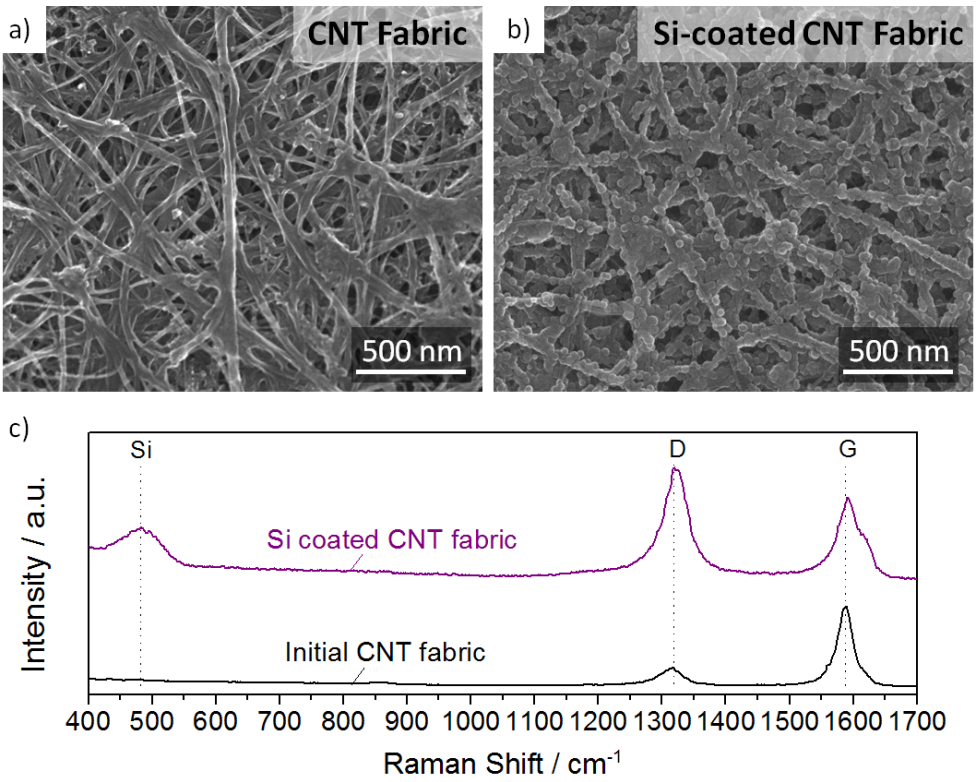

Fig. 20. Microstructural characterization of the CNT fabric before and after Si coating: (a, b) SEM micrographs, (c) Raman spectra.

Flexible electrodes comprised of graphene or carbon nanotubes (CNTs) offer excellent thermal, electrical, and mechanical properties.[21] Graphene paper electrodes have demonstrated very high tensile strength of up to 290 Mpa, however such electrodes suffer from poor cycling ability, very low first cycle coulombic efficiency (CE) of ~12% and low reversible capacity of ~55 mAh/g, metrics much lower than traditional graphite electrodes.[22-23] Insertion of electrolyte solvent molecules in between the individual graphene sheets and their decomposition may explain the observed rapid degradation. One may further expect that mechanical properties of such electrodes should also degrade dramatically after electrochemical cycling. Although tensile tests of individual multi-walled CNTs (MWCNTs) have previously shown tensile strengths > 11 GPa [24], this value is several orders of magnitude higher than the tensile strengths observed for nonwoven CNT fabrics and CNT-polymer composites.[25-28] Commonly reported methods of forming CNT fabrics or buckypapers rely on vacuum filtration of acid-treated CNTs [28-29], impregnation with a polymer [27, 30], or the addition of surfactant [26] to form a fabric with limited size, typically less than a few inches in diameter. In these approaches, howerver, the ability to produce continuous rolls of the CNT fabric/paper with good mechanical strength is very limited. Furthermore, the insertion of electrolyte solvent molecules between the

individual CNTs will likely result in high irreversible capacity losses and low CE at the first cycle combined with a rapid degradation of such CNT electrodes if used as Li-ion battery anodes.

Here we report a route to produce flexible anodes with significantly higher strength and specific capacity than state of the art. Acording to our approach we first produce a high-strength binder-free CNT–based electrically conductive nonwoven fabric and then coat it with a uniform layer of a high capacity material (Figure 19b), such as Si. Performing the deposition of active material on a pre-formed fabric shall allow one to maintain the high electrical and thermal conductivities of the composite because of the elimination of the highly resistive particle-to-particle contacts.[6] In contrast to common CNT fabric assembly methods, we utilize a commercial-scale process through continuous chemical vapor deposition (CVD). This method allows for the scalable production of multifunctional structural materials of various geometries. Si coating is impermeable to solvent molecules and protects the individual CNT-CNT junctions from failure during cycling. Furthermore, by limiting the amount of inserted Li ions we prevented Li from intercalating CNTs, which otherwise would significantly degrade their strength. Indeed, in contrast to previously reported studies [26-28], we show high tensile strength of composite CNT-Si fabric after electrochemical cycling with ultimate tensile strengths (UTS) greater than 90 MPa achieved. The electrochemical performance of the CNT fabric electrodes demonstrated stability for more than 150 cycles.

The as-produced large format, flexible CNT fabric consists of randomly oriented MWCNTs as observed via scanning electron microscopy (SEM, Figure 20 a). A conformal layer of nano-Si was deposited on individual CNTs throughout the fabric (Figure 19 b) via the thermal decomposition of SiH_4. SEM images indicate a thin, uniform coating of ~30 nm thickness was deposited. Although the CNT fabric is relatively thin (~20 μm), the energy density and specific energy of the battery is not significantly compromised due to the incorporation of high capacity Si and the absence of a metal current collector. Raman spectroscopy was performed on the CNT fabric before and after Si coating (Figure 20 c). The initial CNT fabric exhibits two strong Raman peaks ~1320 cm^{-1} and ~1590 cm^{-1}, corresponding to the D-band originating from disordered carbon and the G-band from graphitic carbon, respectively .[31-32] The low value of the ratio of the integrated intensities of the D and G bands, the I_G/I_D ratio, of 0.25, indicates a low defect density in the CNTs.[31-33] After Si coating, a broad Raman band ~480 cm^{-1} associated with hydrogenated amorphous Si emerges [34-35] and the I_G/I_D ratio significantly increases ~1.4, suggesting that Si preferentially deposits on the more disordered sites of the CNT fabric. Further, the free hydrogen produced as a SiH_4 decomposition product can induce surface defects in CNTs, giving rise to higher intensity of the D band.

Electrochemical measurements of the CNT fabric-based electrodes were performed in both pouch and 2016-type coin cell configurations from 0.01 - 1 V Li/Li^+ with a 500 $mAh \cdot g^{-1}$ Li alloying limit against a metallic Li foil counter electrode (Figure 21). Stable performance at C/5 was achieved for > 150 cycles, suggesting good integrity of the composite anode. An average dealloying capacity of 494 $mAh \cdot g^{-1}$, when normalized by the total mass of CNT and Si, and an average coulombic efficiency (CE) ~98% was observed (Figure 21 a). This capacity is over 2.5 times higher than that of commercial electrodes based on graphite-binder mixtures deposited on Cu foils, indicating a good promis for the proposed technology.

Charge/discharge voltage profiles of the Si-coated CNT fabric (Figure 21 b) show transformations in the electrode during cycling. With increased cycling (> 75 cycles), lower overpotentials were observed, indicating an improvement in cycling kinetics. Similarly, cyclic

voltammetry (CV) was performed to further examine the potentials at which Li (de-)alloying occurs (Figure 20 c). A peak at 0.17 V and 0.67 V emerged during lithiation and delithiation, respectively. These values are consistent with previous nanoscale Si-based composite anodes and indicate a high degree of alloying with Si. CV does not show peaks corresponding to intercalation of Li into CNTs, which would degrade their mechanical properties and performance.

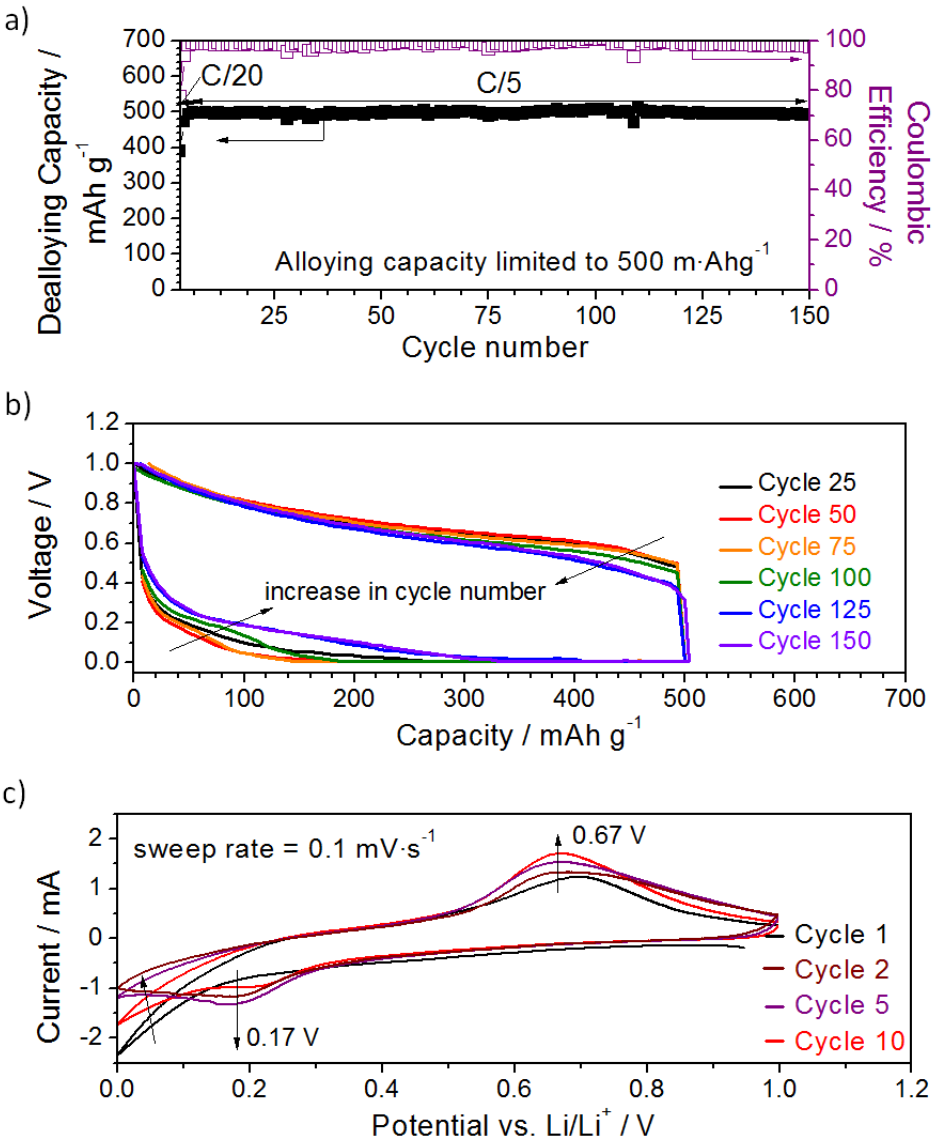

Fig. 21. Electrochemical performance of Si-coated CNT fabric: (a) reversible de-alloying (Li extraction) capacity and Coulombic efficiency versus cycle number, (b) changes in the charge and discharge profiles with cycle number, (c) cyclic voltammograms.

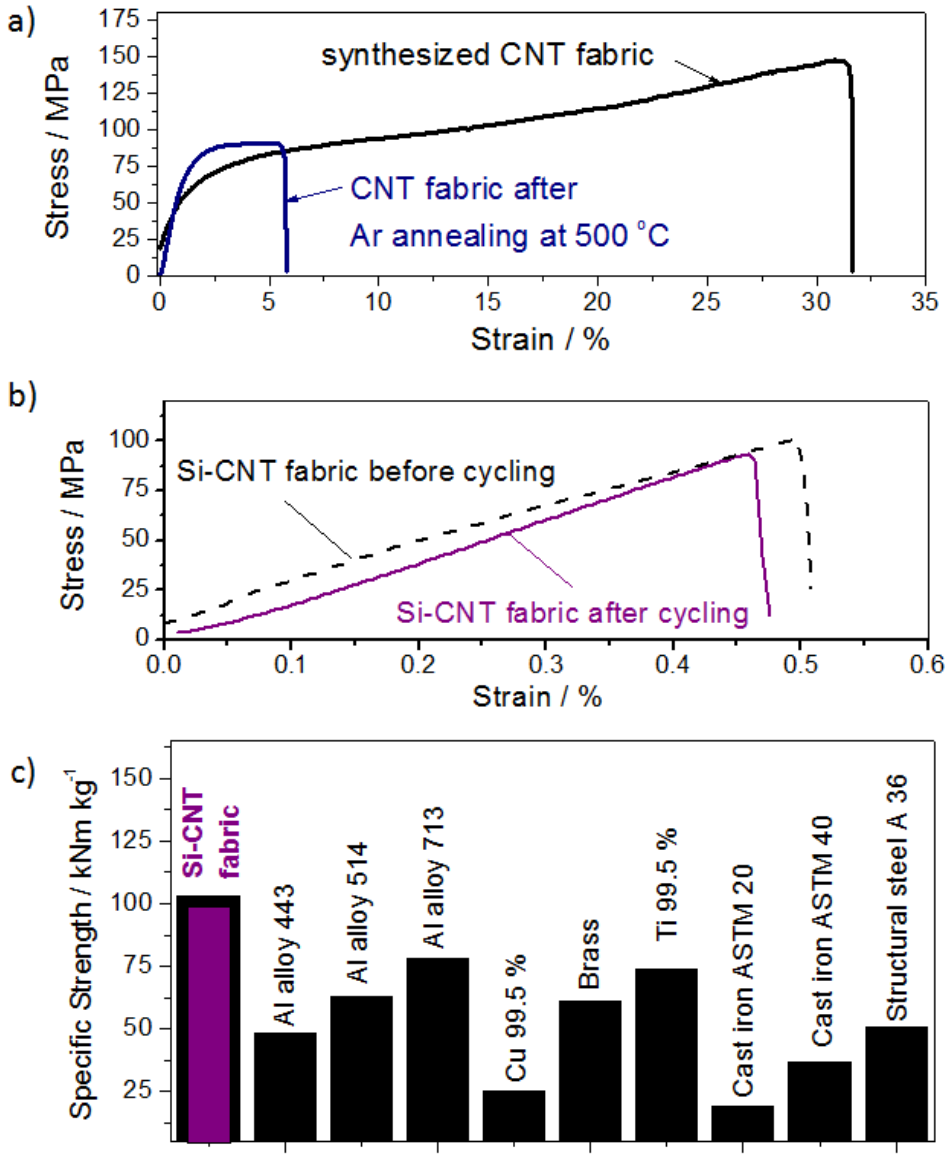

Fig. 22. Mechanical characterization of the produced samples: (a) typical tensile tests on CNT fabric before and after annealing in Ar; (b) typical tensile tests on Si-coated CNT fabric before and after cycling; (c) comparison of the specific strength of the multifunctional Si-coated CNT fabric with that of other common materials.

Uniaxial tensile test experiments were conducted on the CNT fabrics before and after battery cycling. The initial CNT fabric revealed very high maximum elongations of over 30 % and ultimate tensile strength (UTS) value in excess of 150 MPa, comparable to that of cast iron, copper and aluminum alloys [36] (Figure 22a) and up to 5 times higher than previously reported CNT sheets with [27-28] and without polymer [25-26] throughout. Due to the light weight of the fabricated composite fabrics, their specific tensile strength approaches that of structural steel.

As the Si deposition process subjects the electrodes to 500 ^{o}C it is important to study the heating process's impact on the mechanical properties of CNT fabric. Annealing the fabric at 500 ^{o}C in Ar for 1h reduces the maximum alongation to an average value of 6% and the UTS to ~90 Mpa. Longer annealing time does not reduce the fabric mechanical properties any further.

500 °C is not sufficiently high to change the CNT microstructure [37], but sufficient to de-functionalize CNTs. Removing the functional groups from the CNT surface leaves defects behind, which may reduce an axial strength of the individual tubes. [38] In addition, removing these functional groups reduces the Van der Waals interactions between the tubes, which lowers both the maximum alongation and the UTS of the CNT fabric.

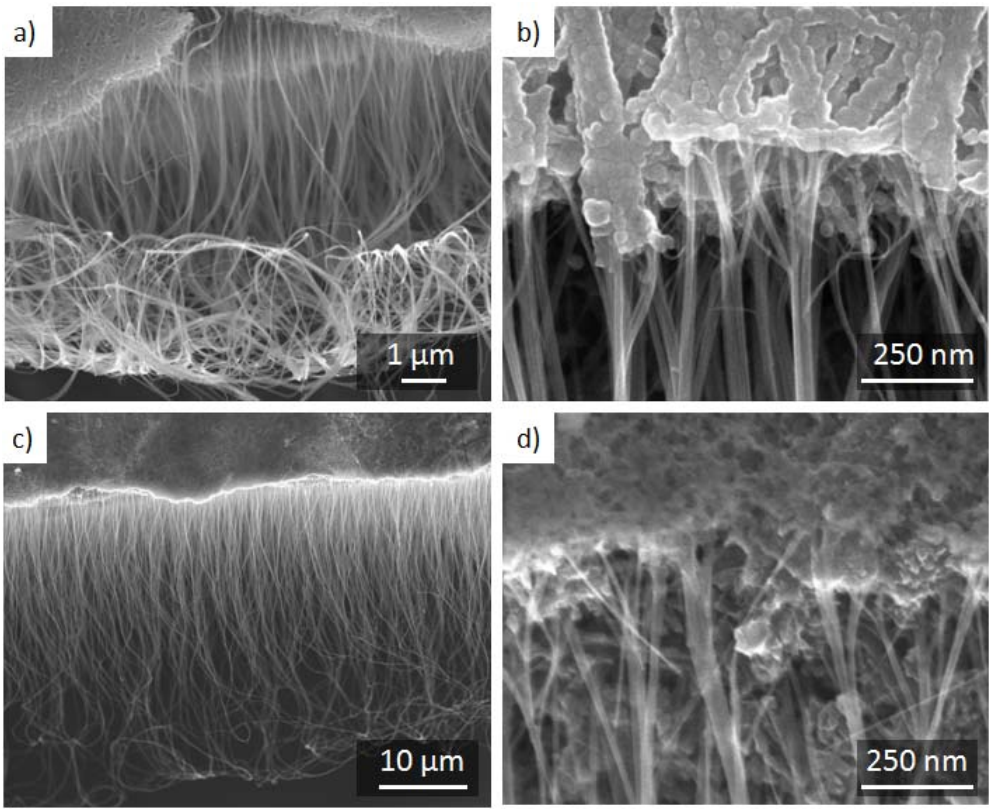

Fig. 23. SEM micrographs of the fracture surface of the Si-coated CNT fabric edge after tensile measurements performed before (a, b) and after (c, d) electrochemical testing.

Si deposition onto the CNT fabric has little effect on the UTS, but decreases its maximum alongation. While selected Si-coated CNT samples demonstrated the UTS of up to 150 MPa and maximum alongation up to 0.8 %, the average values for the UTS and maximum alongations were ~ 100 Mpa and 0.5 %, respectively (Figure 22b). In the as-produced CNT fabric high maximum strain (Figure 22a) and the resultant high fracture toughness was achieved by the energy dissipation during continuous sliding of the Van der Waals bonded individual tubes relatively to each other. Due to the covalent nature of the atomic bonds in Si and its resultant brittle behavior, formation of continuous amorphous Si coating on the internal surface of the CNT fabric could be expected to significantly reduce its ductility. But the experimentally measured composite fabric ductility and the UTS (Figure 22b) was surprisingly relativly high. Indeed, the none-uniformities observed within amoprhous Si coatings (Figure 20b) and the pores within the Si-CNT fabric should act as pre-existing cracks, lowering both the ultimate strength and the maximum alongation achievable in such a composite. SEM studies of the fracture surface (Figure 23) revealed that the high UTS of the Si-CNT fabrics could be attributed to

realignment and the pull-out behavior of CNTs . The fracture edge of the Si-CNT fabric specimens has a clear transition from the randomly oriented CNT fabric to highly aligned CNTs (Figure 23 a, b). We expect that the degree of plastic deformation of the composite fabric could be greatly increased by using active materials having higher ductity than Si (such as Sn or Mg). We further hypothesize that the reduction of the deposition temperature (Figure 22a) could favor achieving better mechanical properties.

Despite volumetric changes of Si during insertion and extraction of Li [39-40], the mechanical properties of the Si-CNT fabric did not degrade significantly after cycling (Figure 4b), demonstrating multi-functional properties of the synthesized fabric. Both the UTS and maximum elongation was reduced by only ~10%. The cycled Si-CNT fabric electrodes demonstrated similar pull-out behavior (Figure 23 c, d). The retention of the fabrics‘ mechanical properties could be explained by avoiding the Li insertion into the individual tubes (Figure 21b, c).

High values of the achieved UTS combined with the low density of Si and C favors the use of the multifunctional Si-CNT fabrics in applications, where high specific strength is essential. Indeed, the specific strength of the synthesized electrodes exceed that of both Cu and Al, conventional current collectors for anodes and cathodes, respectively (Figure 22c). It further exceeds the specific strength of multiple Al alloys, Ti, cast iron and even selected types of structural steel (Figure 22c).

In summary, we fabricated CNT fabric coated with active (Li-ion hosting) materials for use as electrodes for multifunctional Li-ion batteries with high mechanical strength, flexibility and other positive attributes. The investigated example of Si-CNT fabric fabricated via vapor deposition routes demonstrated 2.5 times higher specific capacity than state of the art anodes, stable electrochemical performance for >150 cycles with the capability to retain over 90% of its original strength after cycling. The light weight, good structural stability and high electrical and thermal conductivities of CNTs may allow CNT fabrics to serve as a platform for the generation of novel flexible batteries with enhanced properties and functionalities. We expect that future studies with other active material coatings and deposition methods may allow us to further optimize their performance and achieve even better mechanical and electrochemical properties of the flexible CNT-based electrodes and contribute to the development of high power, flexible and structural batteries.

References

1. Anton, S.R., A. Erturk, and D.J. Inman, *Multifunctional self-charging structures using piezoceramics and thin-film batteries.* Smart Materials and Structures, 2010. **19**: p. 115021-115021.
2. Liu, P., E. Sherman, and A. Jacobsen, *Design and fabrication of multifunctional structural batteries.* JOURNAL OF POWER SOURCES, 2009. **189**(1): p. 646-650.
3. Sun, L., et al., *High-strength all-solid lithium ion electrodes based on Li4Ti5O12.* JOURNAL OF POWER SOURCES, 2011. **196**(15): p. 6507-6511.
4. Thomas, J.P. and M.A. Qidwai, *The design and application of multifunctional structure-battery materials systems.* JOM, 2005. **57**: p. 18-24.
5. Magasinki, A., et al., *High-performance lithium-ion anodes using hierarchical bottom-up approach*

Nature Materials, 2010(in press).

6. Evanoff, K., et al., *Toward Ultra-Thick Battery Electrodes: Aligned Carbon Nanotube - Enabled Architecture.* Advanced Materials, 2011: p. DOI: adma.201103044.
7. Evanoff, K., et al., *Toward Ultra-Thick Battery Electrodes: Aligned Carbon Nanotube – Enabled Architecture.* Advanced Materials, 2011.
8. Kovalenko, I., et al., *A Major Constituent of Brown Algae for Use in High-Capacity Li-Ion Batteries.* SCIENCE, 2011. **334**(6052): p. 75-79.
9. Magasinski, A., et al., *High-performance lithium-ion anodes using a hierarchical bottom-up approach.* Nature Materials, 2010. **9**(4): p. 353-358.
10. Chan, C.K., et al., *High-performance lithium battery anodes using silicon nanowires.* Nature Nano, 2008. **3**(1): p. 31-35.
11. Kasavajjula, U., C. Wang, and A.J. Appleby, *Nano- and bulk-silicon-based insertion anodes for lithium-ion secondary cells.* JOURNAL OF POWER SOURCES, 2007. **163**(2): p. 1003-1039.
12. Kim, H. and J. Cho, *Superior Lithium Electroactive Mesoporous Si@Carbon Core−Shell Nanowires for Lithium Battery Anode Material.* Nano Lett., 2008. **8**(11): p. 3688-3691.
13. Park, M.-H., et al., *Silicon Nanotube Battery Anodes.* Nano Lett., 2009. **9**(11): p. 3844-3847.
14. Wilson, A.M., et al., *Nanodispersed silicon in pregraphitic carbons.* Journal of Applied Physics, 1995. **77**(6): p. 2363-2363.
15. Bridel, J.S., et al., *Key Parameters Governing the Reversibility of Si/Carbon/CMC Electrodes for Li-Ion Batteries.* Chemistry of Materials, 2010. **22**(3): p. 1229-1241.
16. Guo, J.C. and C.S. Wang, *A polymer scaffold binder structure for high capacity silicon anode of lithium-ion battery.* Chemical Communications, 2010. **46**(9): p. 1428-1430.
17. Mazouzi, D., et al., *Silicon Composite Electrode with High Capacity and Long Cycle Life.* Electrochemical and Solid State Letters, 2009. **12**(11): p. A215-A218.
18. Hertzberg, B., J. Benson, and G. Yushin, *Ex-situ depth-sensing indentation measurements of electrochemically produced Si-Li alloy films.* Electrochemistry Communications, 2011. **13**(8): p. 818-821.
19. Evanoff, K., et al., *NanoSi-Coated Graphene Granules as Anodes for Li-ion Batteries.* Advanced Energy Materials, 2011. **1**(4): p. 495-498.
20. Hertzberg, B., A. Alexeev, and G. Yushin, *Deformations in Si-Li Anodes Upon Electrochemical Alloying in Nano-Confined Space.* J. Am. Chem. Soc., 2010. **132**(25): p. 8548-8549.
21. Balandin, A.A., *Thermal properties of graphene and nanostructured carbon materials.* Nat Mater, 2011. **10**(8): p. 569-581.
22. Wang, C., et al., *Electrochemical Properties of Graphene Paper Electrodes Used in Lithium Batteries.* Chem. Mater., 2009. **21**(13): p. 2604-2606.

23. Dahn, J.R., et al., *Mechanisms for Lithium Insertion in Carbonaceous Materials.* SCIENCE, 1995. **270**(5236): p. 590-593.
24. Yu, M.F., et al., *Strength and breaking mechanism of multiwalled carbon nanotubes under tensile load.* SCIENCE, 2000. **287**(5453): p. 637-640.
25. Inoue, Y., et al., *Anisotropic carbon nanotube papers fabricated from multiwalled carbon nanotube webs.* Carbon, 2011. **49**(7): p. 2437-2443.
26. Park, J.G., et al., *Effects of surfactants and alignment on the physical properties of single-walled carbon nanotube buckypaper.* Journal of Applied Physics, 2009. **106**(10): p. 104310-104310.
27. Pham, G.T., et al., *Mechanical and electrical properties of polycarbonate nanotube buckypaper composite sheets.* Nanotechnology, 2008. **19**(32): p. 325705-325705.
28. Zhang, X., et al., *Properties and Structure of Nitric Acid Oxidized Single Wall Carbon Nanotube Films.* The Journal of Physical Chemistry B, 2004. **108**(42): p. 16435-16440.
29. Morris, R.S., et al., *High-energy, rechargeable Li-ion battery based on carbon nanotube technology.* JOURNAL OF POWER SOURCES, 2004. **138**(1-2): p. 277-280.
30. Pushparaj, V.L., et al., *Flexible energy storage devices based on nanocomposite paper.* Proceedings of the National Academy of Sciences, 2007. **104**(34): p. 13574-13577.
31. Antunes, E.F., et al., *Comparative study of first- and second-order Raman spectra of MWCNT at visible and infrared laser excitation.* Carbon, 2006. **44**(11): p. 2202-2211.
32. Tan, P., S. Dimovski, and Y. Gogotsi, *Raman Scattering of Non-Planar Graphite: Arched Edges, Polyhedral Crystals, Whiskers and Cones.* Phil. Trans. R. Soc. Lond. A, 2004. **362**: p. 2289-2310.
33. Ferrari, A.C. and J. Robertson, *Interpretation of Raman spectra of disordered and amorphous carbon.* Physical Review B, 2000. **61**(20): p. 14095-14095.
34. Iqbal, Z. and S. Veprek, *Raman scattering from hydrogenated microcrystalline and amorphous silicon.* Journal of Physics C: Solid State Physics, 1982. **15**(2): p. 377-377.
35. Nguyen, J.J., K. Evanoff, and W.J. Ready, *Amorphous and nanocrystalline silicon growth on carbon nanotube substrates.* Thin Solid Films, 2011. **519**(13): p. 4144-4147.
36. *Mechanical Properties of Materials*, in *CRC Materials Science and Engineering Handbook, Third Edition*, J. Shackelford and W. Alexander, Editors. 2000, CRC Press.
37. Ci, L., et al., *Crystallization behavior of the amorphous carbon nanotubes prepared by the CVD method.* Journal of Crystal Growth, 2001. **233**(4): p. 823-828.
38. Sun, Y.-P., et al., *Functionalized Carbon Nanotubes: Properties and Applications.* Accounts of Chemical Research, 2011. **35**(12): p. 1096-1104.
39. Boukamp, B.A., G.C. Lesh, and R.A. Huggins, *All-Solid Lithium Electrodes with Mixed-Conductor Matrix.* Journal of The Electrochemical Society, 1981. **128**(4): p. 725-729.
40. Obrovac, M.N. and L. Christensen, *Structural Changes in Silicon Anodes during Lithium Insertion/Extraction.* Electrochemical and Solid-State Letters, 2004. **7**(5): p. A93-A93.